ELSEVIER

Biochimica et Biophysica Acta 1328 (1997) 13–29

BIOCHIMICA ET BIOPHYSICA ACTA
BBA

# Evidence from studies of temperature-dependent changes of D-glucose, D-mannose and L-sorbose permeability that different states of activation of the human erythrocyte hexose transporter exist for good and bad substrates

R.J. Naftalin *

*Physiology Group, Division of Biomedical Sciences, King's College London, Strand, London WC2R 2LS, UK*

Received 6 December 1996; revised 7 March 1997; accepted 7 March 1997

**Abstract**

(1) The inhibition constant of L-sorbose flux from fresh human erythrocytes by D-glucose, $K_{i(sorbose)}$ increases on cooling from 50°C to 30°C from $5.15 \pm 0.89$ mM to $12.24 \pm 1.9$ mM; the $K_{i(sorbose)}$ of D-mannose increases similarly, indicating that the process is endothermic. (2) The activation energy $E_{a(sorbose)}$ of net L-sorbose exit is $62.9 \pm 3.1$ kJ/mol; in the co-presence of 5 mM D-glucose $E_{a(sorbose)}$ is reduced to $41.7 \pm 1.6$ kJ/mol ($P < 0.005$). (3) Cooling from 35°C to 21°C decreases the $K_{i(inf.\ cis)}$ of auto-inhibition of D-glucose net exit from $5.2 \pm 0.3$ mM to $1.36 \pm 0.06$ mM; the $K_{i(inf.\ cis)}$ of D-mannose falls from $10.9 \pm 1.65$ mM to $5.7 \pm 0.3$ mM. (4) The activation energy of D-glucose zero-trans net exit is $34.7 \pm 2.1$ kJ/mol and that of D-mannose exit is $69.4 \pm 3.7$ kJ/mol ($P < 0.0025$). (5) The exothermic and exergonic processes of auto-inhibition of D-glucose net exit are larger than those for D-mannose ($P < 0.03$). These data are consistent with D-glucose binding promoting an activated transporter state which following dissociation transiently remains; if an L-sorbose molecule binds within the relaxation time after D-glucose dissociation, it will have a higher mobility than otherwise. Cooling slows the relaxation time of the activated state hence raises the probability that L-sorbose will bind to the glucose-activated transporter. D-Glucose donates twice as much energy to the transporter as D-mannose, consequently produces more facilitation of flux. This view is inconsistent with the alternating carrier model of sugar transport in which net flux is considered to be rate-limited by return of the empty carrier, but is consistent with fixed two-site models. © 1997 Elsevier Science B.V.

*Keywords:* D-Glucose; Erythrocyte; L-Sorbose; Transport; Activated state

## 1. Introduction

Several problems relating to the mechanism of sugar transport remain unexplained. Two of these are:

* Corresponding author. Fax: +44 171 8732286. E-mail: richard.naftalin@kcl.ac.uk


*PII* S0005-2736(97)00062-X

the high $K_i$ of D-glucose-dependent inhibition of L-sorbose net transport across the human erythrocyte membrane [1–6] and secondly, the source from which the energy is obtained to overcome the energy barrier for the return of the empty carrier to complete the net transport cycle [7].

### 1.1. The L-sorbose problem

L-Sorbose is transported via the human erythrocyte D-glucose transporter with an affinity lower by two orders of magnitude than D-glucose (300–500 mM). L-Sorbose transport differs from that of D-glucose as it is neither subject to *accelerated exchange*, nor *counterflow* [1]. Despite the very low affinity of L-sorbose for the Glut 1 transporter, the reported concentration of D-glucose required to inhibit L-sorbose flux by 50% is 2–5-fold higher than the affinity of D-glucose (3–5 mM) for the high-affinity hexose binding sites at the external sites of the transporter [1–6]. This anomalous result still requires an explanation.

LaCelle and Passow [8] suggested that L-sorbose is transported by more than one route. This could explain the high $K_i$ for D-glucose inhibition of L-sorbose flux. In support of this view it was suggested that hydrophobic sugars are more effective inhibitors of L-sorbose than hydrophilic sugars and that L-sorbose may have a second route of transport via the hydrophobic route [9]. However, no strong evidence exists for such an alternative pathway for L-sorbose flux; furthermore, a second route of transport does not account for the absence of any *counterflow* of L-sorbose against D-glucose.

Because the $K_i$ of D-glucose-dependent inhibition of L-sorbose flux has been measured over a wide temperature range, 37–20°C, the comparability of the various measures of $K_i$ for D-glucose is uncertain. Accordingly, it was decided to study the temperature dependence of D-glucose and D-mannose inhibition of L-sorbose net efflux from fresh human erythrocytes systematically over the range 30–50°C. Exit rates of L-sorbose from erythrocytes were obtained photometrically by following the exit from cells preloaded with 100 mM L-sorbose into isotonic saline solutions containing virtually zero L-sorbose [10]. The method is also used to assess how the presence of various concentrations of D-glucose, or D-mannose alters the activation energy of L-sorbose flux.

### 1.2. The relative permeabilities of D-mannose and D-glucose

Since the maximal transport rates $V_m$ of all sugars are deemed to be similar, it is generally assumed that net transport of all high-affinity sugars is rate limited by the slow return of the empty carrier; [3,11–13]. The main factor thought to differentiate transport between sugars is their varying affinity to the transporter. However, a number of observations suggest that this view may be an oversimplification. Jung, Carlson and Whaley [14] observed that the $V_m$ of D-mannose transport in human red cell ghosts at 24°C is only about 30% of that of D-glucose. Also in rat erythrocytes at 24°C the $V_m$ for *zero-trans* net influx of D-mannose is only 20% of that for 3-*O*-methyl-D-glucose, however, the rates of *self exchange*, or *hetero-exchanges* of these sugars were found to be much closer [15]. In contrast, in human erythrocytes at 30°C D-mannose and D-galactose transport are more rapidly transported than D-glucose [4]. It is unlikely that major differences exist in the fundamental modes of sugar transport across the high-affinity glucose transporters, so the explanation for the differences in relative rates of D-mannose and D-glucose transport may lie elsewhere.

Differences in the temperature coefficients of D-mannose and D-glucose permeability could explain the relative differences in transport rates of these two sugars at different temperatures. Accordingly, it was decided to investigate whether the temperature dependencies of D-glucose and D-mannose transport in the temperature range 25–45°C differ. These studies also permit a direct comparison of the activation energies of D-glucose and D-mannose exit and the enthalpies and entropies of interaction of these sugars with the external surface of the transporter. A solution to the related problem of return of the empty carrier to complete the net transport cycle can be obtained from this analysis.

The temperature coefficient of D-glucose transport has been measured several times already. However, no direct comparisons of the temperature coefficients of net movement of more than one sugar are avail-

able. Arrhenius plots of D-glucose and other non-electrolyte fluxes have been shown to be non-linear — a change of slope occurs in the temperature range 20–24°C. This alteration in the temperature coefficient possibly is the result of a phase change in the membrane lipids, or heat capacity of the transporter ($C_p$), or possibly, to unstirred layer effects [3,13,16,17]. In this study, to avoid such complications, sugar fluxes of D-glucose and D-mannose only in the temperature range 25–45°C are used.

## 2. Methods

### 2.1. Solutions

The composition of the buffered saline was as follows in mM: NaCl 140; KCl 2.5; $MgCl_2$ 2.0; Hepes (*N*-2-hydroxyethylpiperazine-*N′*-2-ethanesulfonic acid) 5. All chemicals including L-sorbose, D-glucose and D-mannose were obtained from Sigma Chemical Company, Dorset. The solutions were buffered to pH 7.4 with HCl using appropriate temperature corrections.

### 2.2. Cells

Fresh human erythrocytes were obtained by venepuncture, washed three times in isotonic saline by repeated centrifugation and resuspension. The cells were then suspended in solutions containing sugars at the preloading concentration — usually 100 mM, final haematocrit 10%. The cells were incubated for at least 2 h in the case of D-glucose and D-mannose, or in the case of L-sorbose 5 h, to allow the sugars to equilibrate with the cell water. The cells were then re-centrifuged to obtain a thick cell suspension ca. 95% haematocrit. This cell suspension was kept at 4°C until required. Aliquots of prewarmed cells suspension (7.5 $\mu$l) were added to a 1 $cm^2$ fluorescence cuvette containing 3 ml of saline solution which had been prewarmed to the required temperature. The cell suspensions were mixed vigorously and photometric monitoring was started within 5 s.

### 2.3. Photometric monitoring

The effects of varying equimolar concentrations of D-glucose, or D-mannose, added to both cell water and external solutions, on the exit rates of L-sorbose from cells were monitored photometrically, using a Hitachi 2000-F fluorescence spectrometer with a temperature-controlled and monitored cuvette; $\lambda_{ex} = \lambda_{em} = 650$ nm. The output was recorded and stored directly using a MacLab 2e (AD Instruments). Data were collected at a rate of 1–5 points per second, depending of the time course of exit; each run consists of 200–2000 data points (Fig. 1). The photometric response was found to be approximately linear for osmotic perturbations $\pm 50$ mM NaCl.

The time courses of L-sorbose exit were fitted to mono-exponential curves of the form

$$y_t = A[1 - B \cdot \exp(C \cdot t)]$$

using the curve-fitting program in Kaleidagraph 3.02 (Abelbeck Software); where $y_t$ is the voltage recorded at time $t$; the coefficient $A$ is a scaling factor which fits the curves to the voltage signal, $B$ and $C$ are the exponential coefficients and $t$ is the time in seconds at which $y_t$ is obtained. These fits give correlation coefficients $r > 0.98$. Since the loading concentration of L-sorbose was the same for all experiments (100 mM); the rate coefficient $C$ can be used to monitor the effects of temperature and of either D-glucose, or D-mannose concentration on L-sorbose exit permeability. Complete sets of data, covering the entire temperature range with both D-mannose and D-glucose, were collected over 48-h periods from single blood samples, i.e. ca. 120 flux determinations per session — no obvious deterioration was noted during the sessions.

D-Glucose and D-mannose exit rates were similarly estimated; however, the initial rates of D-glucose and D-mannose exit were then calculated from the following equation: sugar exit rate (mmol $l^{-1}$ cells $s^{-1}$) = $D \cdot C$ (where $D$ = loading concentration − external [sugar]). It should be noted that expression of D-glucose or D-mannose exit as a mono-exponential gives a very good approximation to the initial zeroth order saturation kinetics $r \approx 0.98$. When the external solutions contain a fixed sugar concentration then net exit approximates very closely to a mono-exponential.

### 2.4. FDNB inhibition

The effects of 2,4-dinitrofluorobenzene (2 mM) (Sigma) incubated for 12 h at 5°C with fresh erythrocytes at a 20% haematocrit in the presence of 100

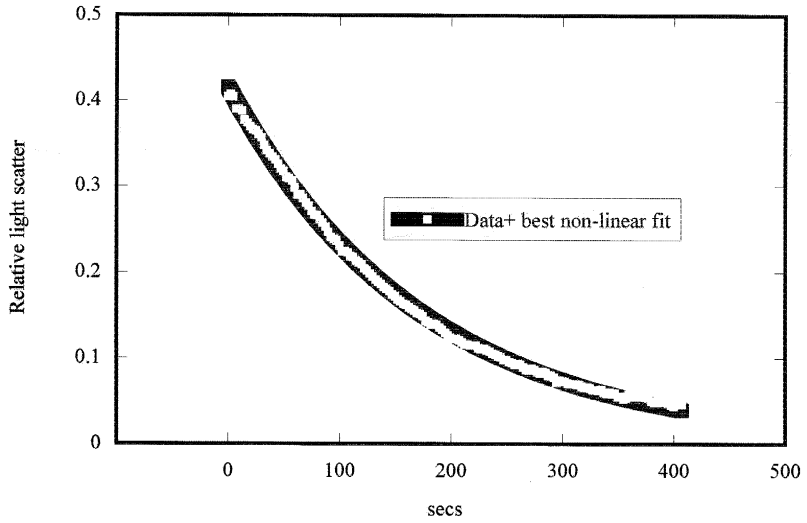


Fig. 1. Example of a data trace showing light scatter changes in a cell suspension of cells loaded with 100 mM L-sorbose at 50°C. The decrease in rate is due to escape of L-sorbose from the cells into the external solution which contains nominally zero L-sorbose. The data are shown in white squares against a black background which is the best-fit line to the data. The equation to the line is: $y_t = A \cdot \exp(B \cdot t)$; where $A = 0.416 \pm 0.0009$; $B = -0.0058 \pm 0.000019$; the regression coefficient to the line is 0.9994.

mM D-glucose on the temperature coefficient of D-glucose exit was monitored. This regimen gives ≈ 99% inhibition of net D-glucose flux [18].

## 3. Results

### *3.1. Effects of temperature on L-sorbose exit rates from fresh human erythrocytes*

An example of L-sorbose exit from fresh human erythrocytes at 50°C is shown in Fig. 1. The scaled data points are fitted to a mono-exponential curve

$$y_t = 1 - B \cdot \exp(-C \cdot t)$$

The fit is almost coincident with the points over the entire time course of exit, $r > 0.999$.

### *3.2. Effects of D-glucose and D-mannose on L-sorbose exit in the temperature range 30–50°C*

The effects of varying concentrations of D-glucose and D-mannose, present at equimolar concentrations in the cell water and external solution, on the rates of L-sorbose exit in the temperature range 30–50°C are shown in Figs. 2 and 3. Both sugars cause a concentration-dependent inhibition of L-sorbose exit. The lines fitting the data are the non-linear least-squares fits obtained using the equation $K_i \cdot V_o/(K_i + S)$; where $K_i$ is the concentration of sugar S giving 50% inhibition of the uninhibited L-sorbose exit rate ($V_o$); $S$ is the equimolar concentration of inhibitor sugar (mM) in the internal and external bathing solutions. The data points represent the means ± S.E.M. ($n \leq 5$ at each temperature; measured with three separate samples of blood from a single donor).

The plots of the effects of temperature on the estimated $K_i$ values of D-glucose- and D-mannose-dependent inhibition of sorbose exit are shown in Fig. 4. The $K_i$ of D-glucose increases from 5.15 ± 0.89 mM at 50°C to 12.24 ± 1.9 mM at 30°C and for D-mannose the $K_i$ increases from 6.96 ± 0.52 mM at 45°C to 12.23 ± 1.9 mM at 30°C. These increases in $K_i$ for both sugars as temperature is reduced are highly significant, as shown by the exponential regression line through the data ($P < 0.001$). These data are also displayed with van't Hoff plots (Fig. 5).

$$\Delta G = -RT\ln K = \Delta H - T\Delta S \text{ or } \ln K = -\Delta H/RT + \Delta S/R$$

where $\Delta G$ is the Gibb's free energy, $K$ is the equilibrium constant $\propto 1/K_m$; hence, the changes in enthalpy $\Delta H$ resulting from interactions of D-glucose and D-mannose with the external surface of the transporter are obtained from the $-(\text{slopes} \cdot R)$ ($R$ = gas constant) of the lines obtained by plotting $\ln(K_{i(\text{inf. cis}}$

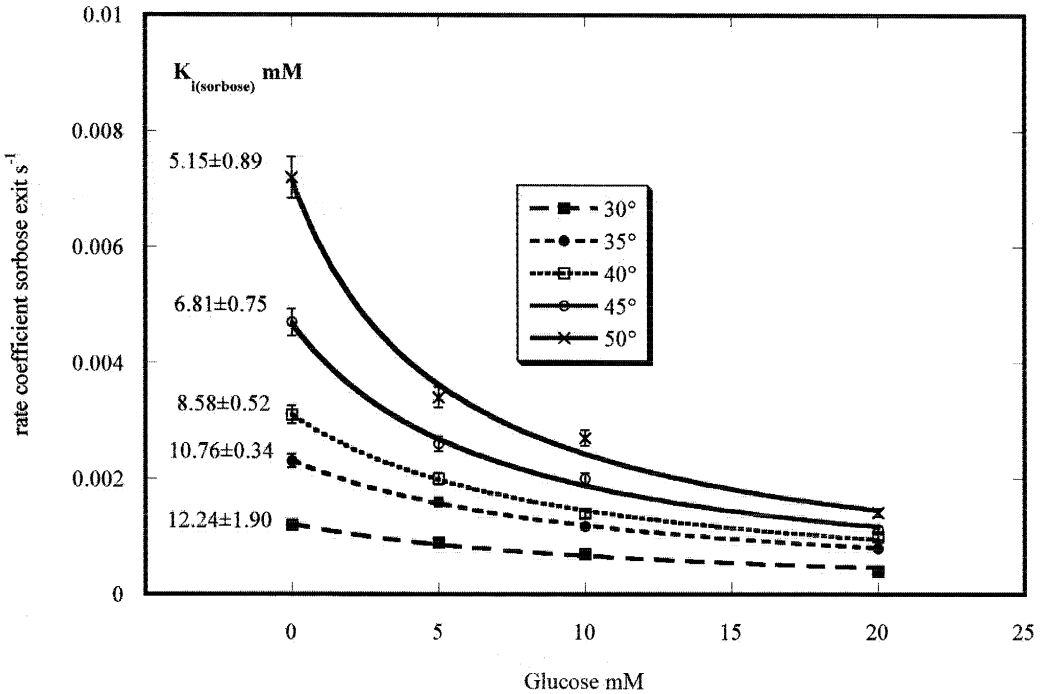


Fig. 2. Effects of temperature and varying concentrations of D-glucose on the rates of L-sorbose exit from human erythrocytes. The lines fitting the data points are the least-squares non-linear fits to the curves $K_i \cdot V_o/(K_i + [S])$; where $K_i$ (mM) is the inhibition constant of sugar S = glucose.

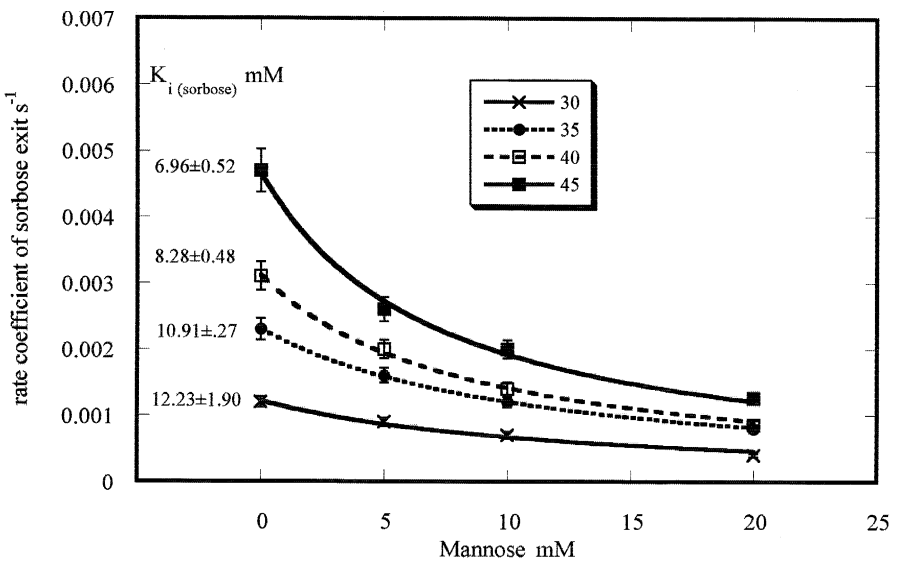


Fig. 3. Effects of temperature and varying concentrations of D-mannose on the rates of L-sorbose exit from human erythrocytes. The lines fitting the data points are the least-squares non-linear fits to the curves $K_i \cdot V_o/(K_i + [S])$; where $K_i$ (mM) is the inhibition constant of sugar S = mannose.

exit) (M)) versus $1/T$ ($K^{-1}$) and the entropies of interaction $\Delta S$ are obtained from the (intercept $\cdot R$) at $1/T = 0$.

The enthalpies $\Delta H$ and the entropies $\Delta S$ of interaction of both D-glucose and D-mannose with L-sorbose transport are not significantly different, although all these parameters differ significantly from zero ($P < 0.01$) (Table 1).

The relatively high temperature coefficients of the $K_i$ values of D-glucose and D-mannose for inhibition of L-sorbose exit explain why such a wide range in the previously reported $K_i$ values of D-glucose inhibition of L-sorbose flux since they were obtained over a range of temperatures.

### 3.3. Activation energy $E_a$ of L-sorbose exit from fresh erythrocytes

The activation energy of L-sorbose exit, $E_a$, is obtained from Arrhenius plots, i.e. ln(rate of L-sorbose exit) vs. $1/T$ ($K^{-1}$)

$$E_a = -\mathrm{d}\ln(\text{rate of L} - \text{sorbose exit})/\mathrm{d}(T \cdot R)$$

In the temperature range 30–50°C, the Arrhenius plots are linear; below this temperature (not shown), some slope change is found, as previously shown for D-glucose exit [3,13,19,20]. The Arrhenius plots of L-sorbose exit and L-sorbose exit with D-glucose (5 and 10 mM); or D-mannose (10 mM) on both sides of the membrane are shown in Fig. 6. The activation energies derived from the Arrhenius plots are displayed in Table 2. The activation energy, $E_a$ of L-sorbose exit is reduced significantly with 5 and 10 mM D-glucose present (Student's $t$-test $P < 0.01$). The activation energy with 10 mM D-mannose present is not significantly different from the activation energy of L-sorbose exit without any other sugar present.

These results reveal that inhibition of L-sorbose exit by D-glucose is not a simple competitive phenomenon, as might be inferred from observation of

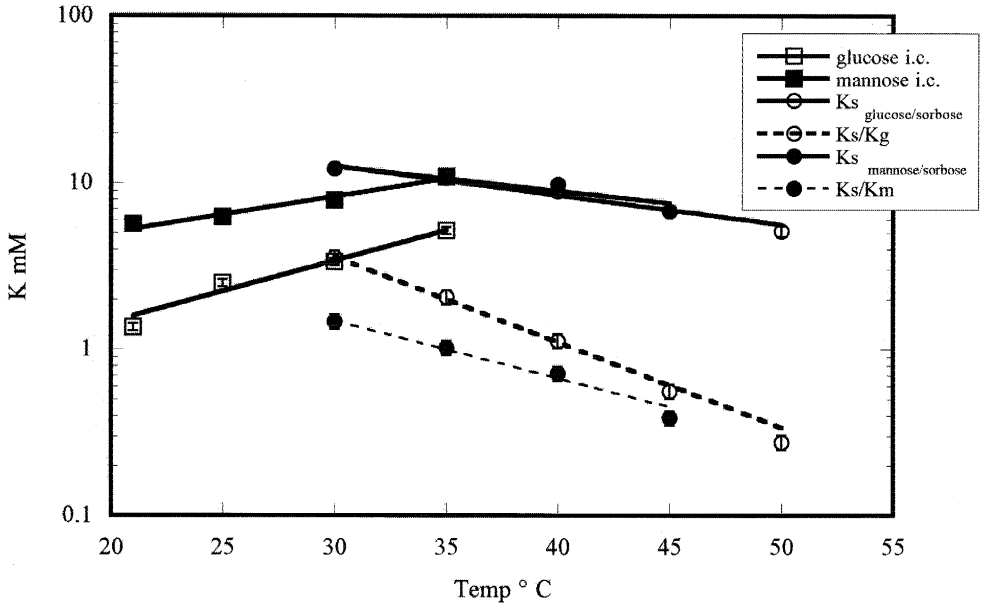


Fig. 4. Effect of temperature on $K_i$ of D-glucose and D-mannose interaction with L-sorbose transport and of auto-inhibition of D-glucose and D-mannose exits. Semi-logarithmic plots of estimates of $K_{i(sorbose)}$ (mM) for D-glucose, open circles, continuous line and $K_{i(sorbose)}$ for D-mannose; closed circles, continuous lines. The data are derived from Fig. 2Fig. 3, respectively, and plotted semi-logarithmically. Semi-logarithmic plots of the estimates of $K_{i(inf.\ cis)}$ (mM) for auto inhibition of D-glucose (open squares and continuous line) and D-mannose (filled squares and continuous line). Semi-logarithmic plots of the estimates of the normalised $K_{i(sorbose)}/K_{i(inf.\ cis)}$ for D-glucose (open circles, dotted line) and D-mannose (filled circle, dotted lines). The lines fitting the data points are the exponential regression lines. $y_T = A \cdot \exp(B \cdot T)$; where $A$ and $B$ are the exponential coefficients and $T$ is the temperature (in °C).

Table 1
Thermodynamic parameters obtained from van't Hoff plots of infinite-cis exits of D-glucose, D-mannose and their inhibition of net L-sorbose net exit

| | $\Delta H$ (kJ/mol) | $P$ | $\Delta S$ (J/K per mol) | $P$ |
|---|---|---|---|---|
| $Mannose_{(inf.\ cis)}$ | $-35.1 \pm 4.7$ | | $-76.0 \pm 15.5$ | |
| $Glucose_{(inf.\ cis)}$ | $-68.7 \pm 8.6$ | $< 0.027$ | $-179.6 \pm 29.1$ | $< 0.030$ |
| $Mannose_{(sorbose)}$ | $29.8 \pm 7.3$ | | $134.4 \pm 28.7$ | |
| $Glucose_{(sorbose)}$ | $35.6 \pm 3.6$ | n.s | $153.0 \pm 11.5$ | n.s |
| $Mannose^{n}_{(sorbose)}$ | $69.7 \pm 7.6$ | | $226.1 \pm 24.6$ | |
| $Glucose^{n}_{(sorbose)}$ | $104.5 \pm 4.3$ | $< 0.017$ | $333.4 \pm 13.9$ | $< 0.020$ |

The parameter values are presented as mean ± S.E.M. All significance levels refer to the differences between D-glucose and the D-mannose parameter in the row above. $Glucose^{n}_{(sorbose)}$ refers to parameters for reduced or normalised glucose concentration, i.e. $glucose_{(sorbose)}/glucose_{(inf.\ cis)}$; $glucose_{sorbose}$ refers to concentration of glucose giving 50% reduction of L-sorbose exit. D-$Glucose_{(inf.\ cis)}$ refers to glucose concentration in external solution giving 50% reduction in D-glucose exit.

D-glucose, or D-mannose-dependent inhibition of L-sorbose flux at a single temperature.

### *3.4. Comparison of the activation energies of D-glucose and D-mannose exit via the hexose transporter in fresh human erythrocytes*

The initial rates of *zero-trans* exit of D-glucose and D-mannose from cells loaded with 100 mM sugar into solutions containing nominally zero D-glucose (final concentration ≈ 0.25 mM) are displayed as functions of temperature in the range 20–40°C (Fig. 7). Each point is the mean ± S.E.M. ($n \leq 6$ at each temperature; measured with three separate samples of blood from a single donor). At temperatures below 32°C *zero-trans* exit of D-mannose is slower than D-glucose exit; whereas, above 32°C, D-mannose exit is faster than exit of D-glucose. This result demon-

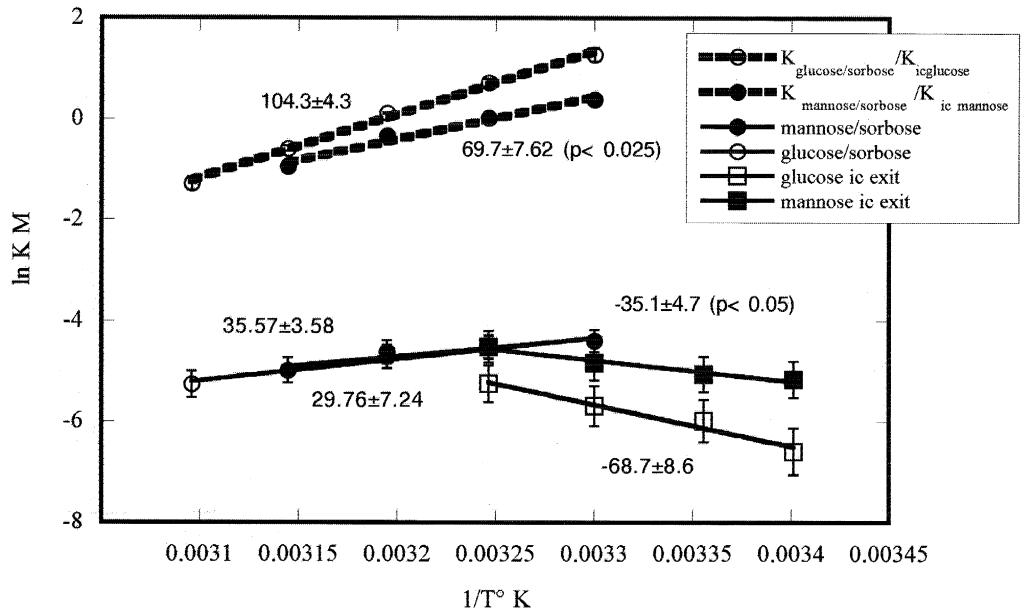


Fig. 5. Van't Hoff plots of estimates of D-glucose and D-mannose interactions with sorbose transport and also auto-inhibitions. $K_{i(sorbose)}$ for D-glucose (open circles, continuous line) and $K_{i(sorbose)}$ for D-mannose (closed circles, continuous lines). The data are derived from Fig. 2Fig. 3, respectively, and plotted as van't Hoff plots $\ln(K_i\ (M))$ versus $1/T$ ($T$ in K). Van't Hoff plots of the estimates of $\ln(K_{i(inf.\ cis)}\ (M))$ for auto-inhibition of D-glucose (open squares and continuous line) and D-mannose (filled squares and continuous line). Plots of the estimates of the normalised $\ln(K_{i(sorbose)}/K_{i(inf.\ cis)})$ for D-glucose (open circles, dotted line) and D-mannose (filled circle, dotted lines). The lines fitting the data points are the linear regression lines. The slopes and intercepts of these lines are used to derive the enthalpy and entropy changes due to auto-inhibitions of D-glucose and D-mannose flux and their interactions with L-sorbose flux (Table 1).

Table 2
Activation energies derived from Arrhenius plots of net sugar

| | $E_a$ (kJ/mol) | $P$ | d.f. |
|---|---|---|---|
| L-Sorbose exit | 62.9 ± 3.1 | | 3 |
| L-Sorbose exit + D-glucose 5 mM | 41.7 ± 1.6 | < 0.005 | 3 |
| L-Sorbose exit + D-glucose 10 mM | 42.8 ± 7.0 | < 0.05 | 3 |
| L-Sorbose exit + D-mannose 10 mM | 54.8 ± 6.5 | n.s. | 3 |
| D-Glucose$_{(inf.\ cis\ exit)}$ | 34.7 ± 2.1 | | 3 |
| D-Mannose$_{(inf.\ cis\ exit)}$ | 69.4 ± 3.7 | < 0.0025 | 3 |

d.f. = $n-2$; $n$ = number of temperature conditions; each condition is the pooled mean of six or more separate estimates of rate from three separate blood samples. The significance of differences between L-sorbose alone and L-sorbose with added sugar and between D-glucose and D-mannose fluxes.

strates qualitatively that the temperature coefficient of D-mannose exit is higher than that of D-glucose.

Arrhenius plots of the pooled data in Fig. 7 are displayed in Fig. 8 and Table 2. The activation energy of *zero-trans* D-mannose exit is double that of D-glucose (Student's *t*-test $P < 0.0025$).

### 3.5. Effect of 2,4-dinitrofluorobenzene, FDNB on the activation energy of D-glucose$_{(zero\text{-}trans)}$ exit

Incubation of human erythrocytes with 2 mM FDNB in the presence of 100 mM D-glucose for 12 h at 4–5°C (see Section 2) has a very large inhibitory effect on D-glucose exit (> 99%). Nevertheless, as D-glucose exit is very fast in the temperature range 20–40°C, it is still possible to observe the residual rate of D-glucose exit from the FDNB-treated cells. The Arrhenius plot of D-glucose exit from FDNB-treated cells is displayed in Fig. 8. Although the absolute rate of D-glucose exit is inhibited by a constant factor in the range of temperatures measured, the activation energy of D-glucose exit = 40.5 ± 0.62 kJ/mol is almost unaffected in comparison to D-glucose exit from control cells = 34.7 ± 2.1 kJ/mol

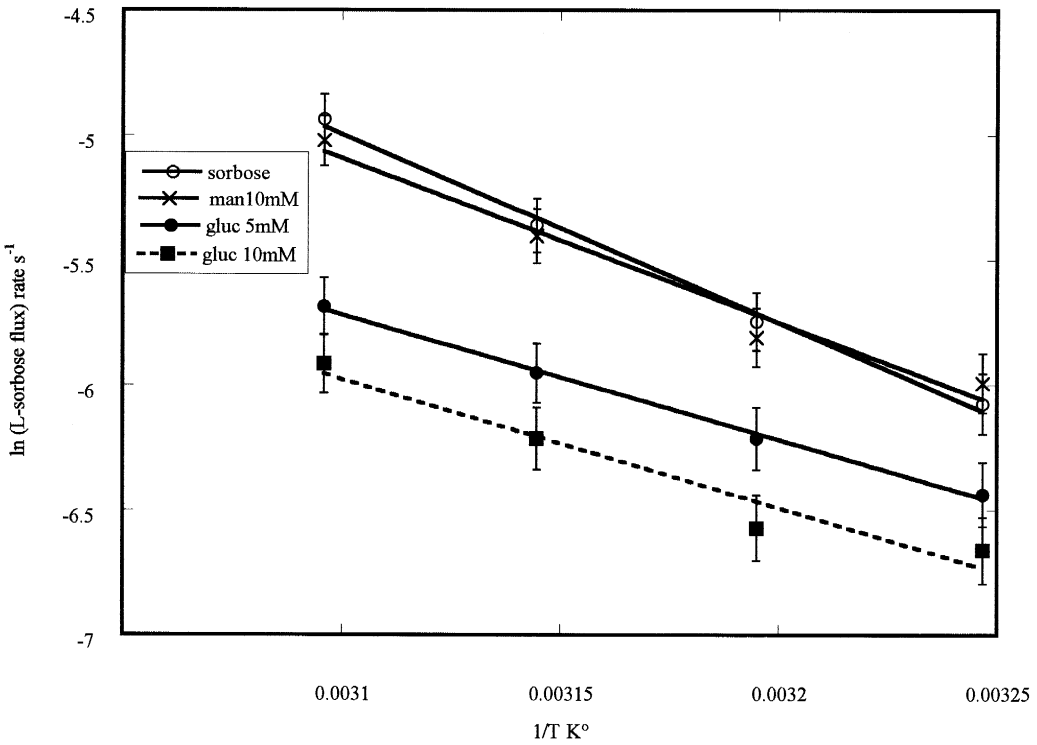


Fig. 6. Arrhenius plots of L-sorbose exit from human erythrocytes. L-Sorbose alone (open circles continuous line); 5 mM D-glucose (filled circles continuous line); 10 mM D-glucose (filled squares, dotted line) or with 10 mM D-mannose present (crosses with continuous line). The error bars are S.E.M. of six or more separate determinations of rate from three different samples of blood from the same donor. The activation energies estimated from the slopes of the lines are shown in Table 2.

(n.s.). This result confirms earlier work of Dawson and Widdas [19], who also observed no change in the temperature coefficient of net D-glucose exit following inhibition by FDNB. This result indicates that even when the great majority of the transporters are inactivated, the residual activity of the transporter is unaffected.

### 3.6. Effect of temperature on the K(inf. cis exit) of D-glucose and D-mannose

As the classic experiments of Sen and Widdas [3] demonstrated, the initial rate of D-glucose exit from cells loaded with saturating concentrations of D-glucose is slowed by the presence of D-glucose in the external solution. The $K_{(\text{inf. cis exit})}$ of D-glucose decreases on cooling in the range 45°C–2.0°C. In this present study the effects of a narrower range of temperature on the $K_{(\text{inf. cis exit})}$ of both D-glucose and D-mannose exit are measured (Fig. 4). The $K_{i(\text{inf. cis})}$ of both D-glucose and D-mannose falls with cooling from 35°C to 21°C; however, the temperature sensitivity of D-glucose $K_{i(\text{inf. cis})}$ is twice that of D-mannose.

A replot of the *infinite-cis* exit data as van't Hoff plots shows that both enthalpies and entropies of D-glucose interaction with the external site of the transporter are nearly twice those of D-mannose (Fig. 5, Table 1).

### 3.7. Estimation of the reduced or normalised enthalpies of D-glucose and D-mannose interaction with L-sorbose transport

The dissociation constants of interaction of D-glucose and D-mannose with L-sorbose transport are virtually the same and increase as temperature is reduced. However, as shown in Section 3.6, cooling increases the binding affinities of D-glucose and D-mannose to the transporter, but to different extents. A correction must be applied to obtain estimates of the enthalpies and entropies of D-glucose and D-mannose interaction with L-sorbose transport which are independent of temperature-induced changes in sugar

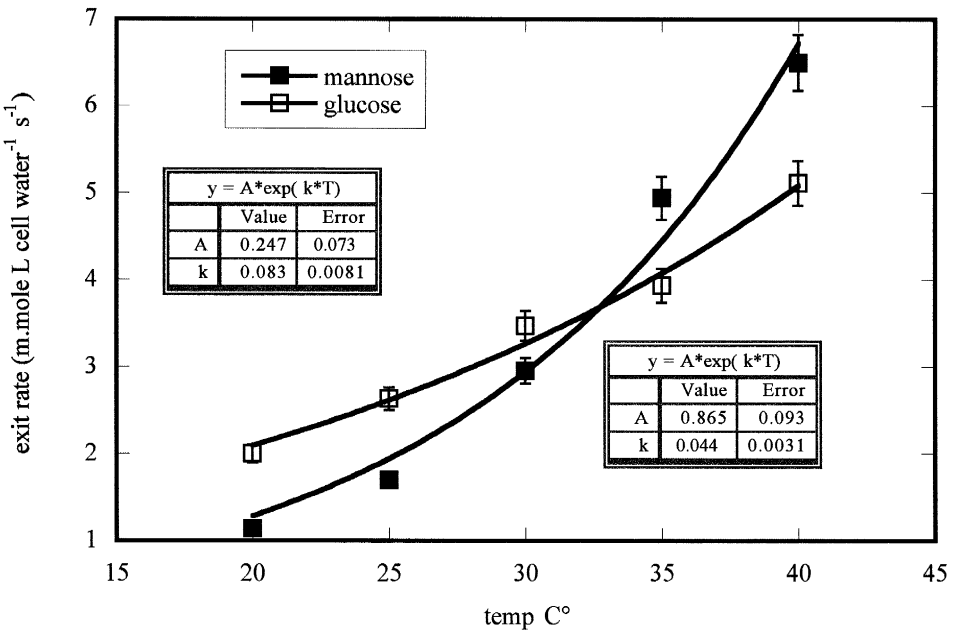


Fig. 7. Comparison of *zero-trans* exit rates of D-glucose and D-mannose from fresh human erythrocytes over a range of temperatures. The lines fitting the data points are the exponential regression lines of the form $y = A \cdot \exp(kT)$, where $A$ and $k$ are the exponential regression parameters and $T$ is the temperature in (°C). The value of the parameter $A$ for D-mannose is $0.247 \pm 0.073$ and for D-glucose, $A = 0.865 \pm 0.093$ ($P < 0.01$, two-tailed Student's $t$-test) and $k$ for D-mannose is $0.044 \pm 0.0031$ and for D-glucose $k = 0.083 \pm 0.0081$ ($P < 0.011$, two-tailed Student's $t$-test). The error bars are the S.E.M. of six or more estimates of exit from three separate blood samples.

affinity ($K_{(\text{inf. cis})}$). A way of correcting for the effects of temperature on the $K_{i(\text{sorbose})}$ is to use the reduced affinity: $K^T_{i(\text{sorbose/glucose})}/K^T_{(\text{inf. cis exit D-glucose})}$.

Because L-sorbose moves across the erythrocyte membrane slowly, it is inconvenient to monitor L-sorbose fluxes using the photometric method below 30°C; it is also difficult to monitor the fast rates of D-glucose and D-mannose fluxes photometrically much above 45°C; hence, there is little overlap between the ranges of measurement of D-glucose and L-sorbose exits. Nevertheless, by using the exponential regression coefficients obtained from the fits to the results in Fig. 4, it is possible to estimate $K_{i(\text{inf. cis exit})}$ for D-glucose/D-mannose in the temperature range 40–50°C. By plotting the relationship

$$\ln K^{T_{i(\text{sorbose/glucose})}}/K^{T_{(\text{. cis exit D-glucose})}} \text{ versus } 1/T \ (\text{K}^{-1})$$

and similarly for D-mannose, additional van't Hoff plots of the reduced (normalized) affinities are obtained (Fig. 5).

Whilst both relationships indicate large negative enthalpies, (endothermy) of D-glucose/D-mannose interaction with L-sorbose transport, as with the uncorrected responses, there is a significant difference between the normalized enthalpies, $\Delta H^n$ of D-glucose and D-mannose interaction with the L-sorbose transporter ($P < 0.025$). Similarly, the normalized entropy, $\Delta S^n$ of D-glucose interaction with L-sorbose also exceeds that of D-mannose ($P < 0.02$) (Table 1).

These results corroborate the finding that D-glucose has a much greater influence than D-mannose on the activation energy $E_a$ of L-sorbose exit (Table 2).

## 4. Discussion

The following new results have been obtained with L-sorbose.

The $K_{i(\text{sorbose})}$ values of both D-glucose- and D-mannose-dependent inhibition of L-sorbose exit de-

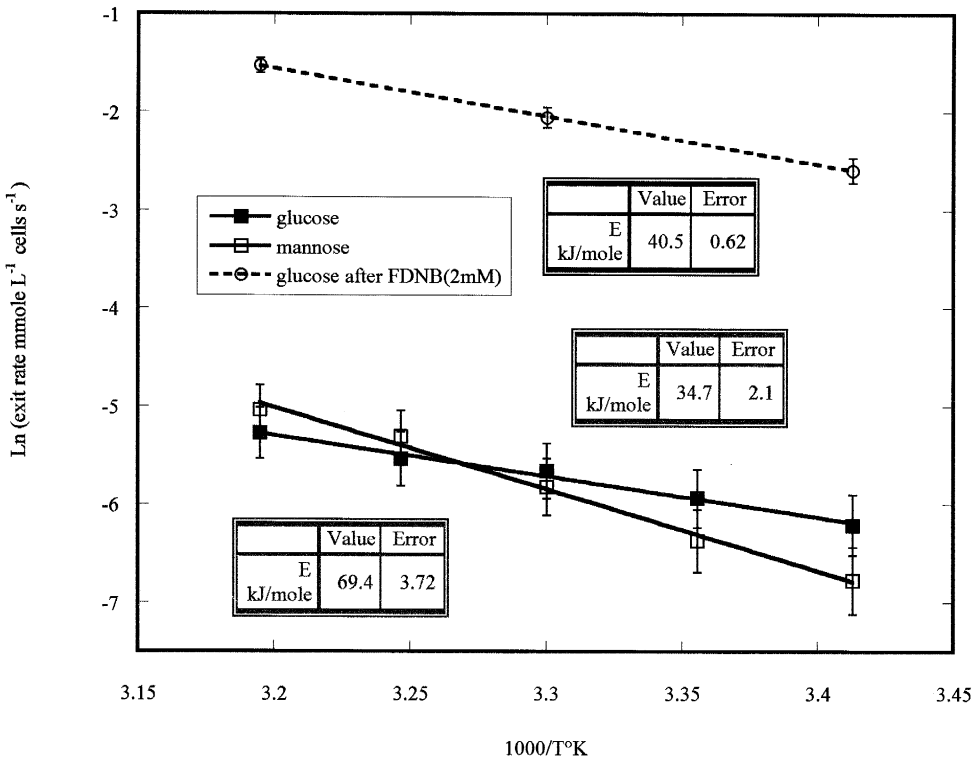


Fig. 8. Arrhenius plots of *zero-trans* exit of D-glucose and D-mannose from fresh human erythrocytes. The activation energies $E_a$ values derived from these plots are displayed in Table 2. The plot also shows the activation energy of D-glucose exit from cells inhibited following incubation with FDNB (2 mM) + 100 mM D-glucose. There is no significant change in the $E_a$ of D-glucose exit following FDNB inhibition.

crease as the temperature is raised in the range 25–50°C (Fig. 4) indicating that both sugar interactions with sorbose transport are endothermic (Fig. 5, Table 1). Small, but significant, endergonic interactions of D-glucose and D-mannose with L-sorbose transport are also obtained ($P < 0.01$).

The increases in $K_i$ for inhibition of L-sorbose exit by both D-glucose and D-mannose on cooling are anomalous. These results contrast with the 'normal' exothermic and exergonic reductions in the $K_{(\text{inf. cis exit})}$ values of D-glucose and D-mannose with cooling (Fig. 4). The temperature-corrected van't Hoff plots are also shown in Fig. 5. These normalized enthalpies and entropies of D-glucose and D-mannose interaction can also be obtained from the following relations

$$\Delta H^{n(\text{sorbose})} = \Delta H_{(\text{sorbose})} - \Delta H_{(\text{inf. cis})}$$

and similarly

$$\Delta S^{n(\text{sorbose})} = \Delta S_{(\text{sorbose})} - \Delta S_{(\text{inf. cis})}$$

The normalized results estimated by this means are virtually identical to those obtained by extrapolation using the fits from the results in Fig. 4 (Table 1).

(1) The results indicate that the L-sorbose *extracts* energy from the transporter during transport; double with D-glucose present compared with D-mannose; whereas, the results with the auto-interactions of D-glucose and D-mannose indicate that D-glucose *donates* twice as much energy as D-mannose to the transporter during binding to the transporter.

(2) These results above are corroborated by observations showing that the activation energy $E_a$ of L-sorbose exit is significantly reduced with D-glucose 5 mM present, but not with D-mannose (10 mM) present (Table 2).

The other results revealed by this study are:

(3) The higher activation energy, $E_{a(\text{D-mannose})}$ is greater than $E_{a(\text{D-glucose})}$ ($P < 0.01$)) (Table 2).

This finding elucidates the previously perplexing results that the maximal rate of D-mannose net flux at 24°C is only 20% of the 3-*O*-methyl-D-glucose flux in rat erythrocytes [15]. It also confirms the observations by Jung et al. [14] that D-mannose permeability in human red cell ghosts is 70% less than that of D-glucose at 24°C; whereas at 30°C the galactose and D-mannose exits are faster than the D-glucose exit from human erythrocytes [4].

The $E_{a(\text{D-glucose})}$ for *net* exit observed in this study is similar to that found by Sen and Widdas [3] over the same temperature range. As the comparisons of D-mannose and D-glucose in this present study were always made with paired observations using erythrocytes from the same donor, it is likely that the observed differences in $E_a$ between these sugars are real.

(4) The observation that the $E_{a(\text{D-glucose})}$ *zero-trans* exit $= 40.5 \pm 0.6$ kJ/mol in cells whose D-glucose transport system is more that 99% inhibited by pretreatment with FDNB is almost unaltered (Fig. 8) confirms previous findings by Dawson and Widdas [19]. This illustrates the fundamental point that $E_a$ relates to the intensive permeability of the D-glucose transporter and is independent of the number of transporters operating in parallel.

### *4.1. Evidence negating the view that return of the empty carrier is rate-limiting for sugar transport*

An important consequence of the large difference in activation energy *of zero-trans* net exit of D-glucose and D-mannose (Table 1) is that it negates the hypothesis that the rate of return of the empty carrier determines the rate of net sugar exit in the temperature range 20–30°C [7]. If the rate of return of the empty carrier controlled net sugar exit, then: the activation energies $E_{a(\text{D-glucose})}$ and $E_{a(\text{D-mannose})}$ of *zero-trans* net exits should be similar, i.e. related to the activation energy of movement of the empty carrier alone: and the $V_{max}$ values of exit of the two sugars should be similar over a wide temperature range. However, the $V_{max}$ values of D-mannose and D-glucose exits from human erythrocytes are only similar within a narrow temperature range 30–35°C, above this temperature, or below it, they differ significantly (Fig. 7).

Below 30°C, *exchange exit* rates of D-glucose are faster than are *net exit* rates [1,13,21,22]. Similarly exchange rates of D-mannose are faster than net flux of D-mannose [14,15]. It is deduced from this on the basis of the alternating carrier model that return of the empty carrier rate limits the net transport cycle [1,4,7,13]. However, since in this temperature range D-mannose exit is slower than D-glucose exit, it follows that return of the empty carrier cannot be a controlling factor for net D-glucose exit and that an alternative explanation for the different rates of net exit of the two sugars is required.

If it were proposed that the return of the D-mannose-loaded carrier is rate-limiting, but that D-glucose exit is controlled by the return of the empty carrier then mannose *exchange* should be much slower than that of D-glucose — however, this is not the case [3,14,15].

### *4.2. A fixed-site model for sugar transport in accord with the thermodynamic data*

The permeabilities of organic solutes across erythrocyte membranes are inversely related to their activation energies $E_a$ [16,17]. The D-glucose-dependent reduction in the $E_{a(\text{L-sorbose})}$ exit (Table 2) indicates that it facilitates the movement of L-sorbose across the transporter. However, this effect on L-sorbose exit is not manifest as an overt increase in L-sorbose permeability. Because of the large differences in affinities of D-glucose, D-mannose and L-sorbose, both D-glucose and D-mannose reduce the net L-sorbose flux overall.

The lower activation energy $E_a$ for D-glucose net exit, than for D-mannose or L-sorbose (Table 2), indicates that the hexose transporter adopts conformations which favour the passage of D-glucose more than either D-mannose, or L-sorbose.

The higher enthalpy and entropy changes following D-glucose$_{(\text{inf. cis})}$ auto-interaction with the transporter compared with the change following D-mannose$_{(\text{inf. cis})}$ interaction, ($P < 0.03$) (Table 1) suggest that the lower activation energy of net movement of D-glucose compared with D-mannose (Table 2) is a consequence of the larger binding force $\Delta H_{(\text{D-glucose})}$ which produces a larger conformation change $\Delta S_{(\text{D-glucose})}$ than obtained with D-mannose. The model also implies that energy donated to the transporter by D-glucose or D-mannose is transferred to L-sorbose in the interval between successive ligand transits through the transporter.

Net exit of sugar can be considered as a multistep process: (Stage 1) a sugar-induced conformational change at the inner fixed transporter site which displaces the transporter from a ground state to an activated state, thereby permitting Stage 2; (Stage 2) a rapid translation of the sugar through the transporter to the outer site, where (Stage 3) a similar conformational change occurs leading to dissociation of sugar from the external site. Flux to the external solution at Stage 3 completes the net transport process, whilst leaving the transporter transiently in an activated state (Scheme 1).

A second molecule passing through the transporter in quick succession to the first, will experience less resistance; since the sites on both sides of the transporter are in a receptive, or primed condition requiring lesser, conformational changes to facilitate transport (Scheme 1, Stage 4b).

The results in Tables 1 and 2 support the view that there is hysteresis, or a short term memory of the intaglio imprint made by the most recently dissociated hexose on the transporter; whose extent on L-sorbose transport is related to the strength of interactions with the alternate ligand (Tables 1 and 2). A transported solute which does not bind strongly at the Stage 1, e.g. L-sorbose, does not induce a large conformational change, therefore does not induce any facilitatory effects; hence, the activation energy $E_a$ for net flux of L-sorbose is higher than for D-glucose.

This two-site mechanism of sugar transport differs crucially from the one-site model as it requires no second stage where empty sites return from *trans* to *cis* sides to complete the transport cycle: therefore the problem of accounting for the energy source for this hypothetical process is avoided [7].

### *4.3. Estimation of the rate of energy transference between the D-glucose and L-sorbose*

At 40°C 100 mM D-glucose exits from the cells completely within 20 s. There are $1 \times 10^{13}$ human red cells per litre and approximately $(2-4) \times 10^5$ D-glucose transporters per cell [23,24]; i.e. $4.0 \times 10^{18}$ transporters per litre cells. Hence, $0.1 \times 6.02 \times 10^{23}$ D-glucose molecules leave the cells in 20 s that is $3 \times 10^{21}$ molecules per s per litre cells; or 750 D-glucose molecules per transporter per s. Thus, the average time interval between successive D-glucose molecules crossing each transporter is 1.3 ms.

When [D-glucose] = 5 mM and net transport rate is approximately half maximal the interval between successive net transport events is 2–3 ms; equilibrium exchange transport of D-glucose (5 mM) is slightly faster; i.e. the interval between exchange transport transits $\approx$ 1–2 ms.

At 40°C the time interval between successive L-sorbose molecules crossing a hexose transporter with

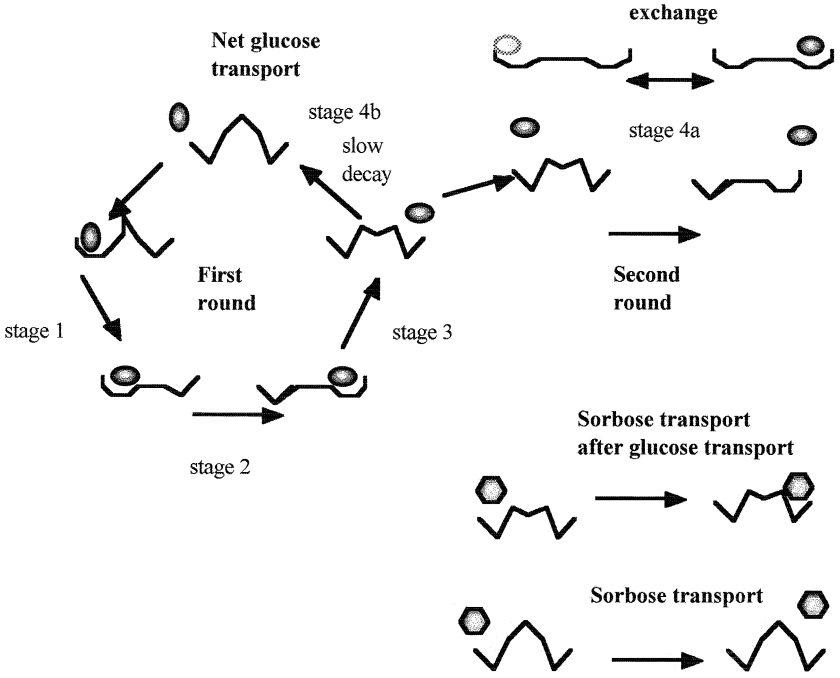


Scheme 1. Diagram showing the glucose-induced conformation changes in the transporter and the effects of short term memory of ligand-induced change on subsequent transport events. The diagram shows the stages of net glucose transport. In stage 1 glucose is 'recognised' by the transporter and effects a conformational change in the the transporter (cis side); stage 2 shows the net transport step with a conformational change on both cis and trans sides; stage 3 shows the dissociation of glucose from the transporter with either stage 4b a slow return to the resting ground state of the transporter or to stage 4a a second glucose molecule binds to the primed cis side of the transporter and experiences less resistance in transit across the transporter or the transporter binds a second sugar at cis and trans sites which can take part in exchange with even less resistance to transit. The diagram also shows that sorbose transit experiences more resistance than glucose as it does not alter the transporter conformation as much as glucose; however, if it reacts with a transporter which has recently encountered glucose, transit resistance to sorbose is reduced.

D-glucose absent is 40–50 ms; with 5 mM D-glucose present, the interval increases to 80–100 ms. Since L-sorbose has a negligible effect on D-glucose transport, it follows that passage of a single L-sorbose molecule with D-glucose 5 mM present on both sides, must occur in the interval between successive transits, net or exchange, of D-glucose; i.e. $< 1$ ms. It follows the energy transference between D-glucose and L-sorbose must take place during this time interval.

The divergence of $K_{(\text{inf. cis})}$ and $K_{i(\text{sorbose})}$of D-glucose and D-mannose is only observed below 35°C (Fig. 4); i.e. there is no evidence of significant energy transference between D-glucose and L-sorbose above 35°C. As the interval between successive D-glucose transits increases with cooling, it follows that the energy donated to the transporter by interaction with D-glucose and D-mannose must be retained by the transporter for longer intervals, at temperatures below 30°C $>$ 2–5 ms.

### *4.4. An explanation for the anomalous temperature response of the $K_i$ of D-glucose and D-mannose-dependent inhibition of L-sorbose flux*

Fluorescence studies [25–28], have shown that when D-glucose binds to Glut 1 transporter there is an initial very fast reaction $t_{1/2} \ll 1$ ms, followed by a slower series of reactions ($t_{1/2} \cong 1$–10 ms), observable using stopped-flow fluorescence. These changes, due to rearrangements of the tryptophan residues in Glut 1, which are inhibited by cytochalasin B, have been interpreted as being consistent with translocation of an alternating carrier complex from inside to

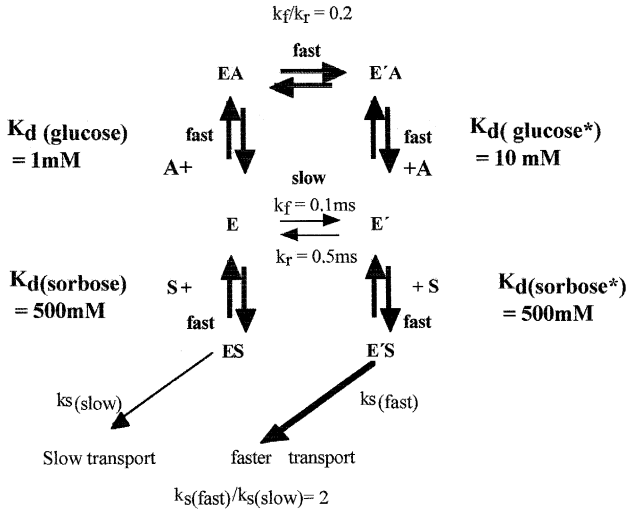


Scheme 2. A model of a sugar transporter with a short term memory for the dissociated ligand.

outside facing conformations [25–27]. However, Janoshazi and Solomon [28] suggest that they do not necessarily imply such a specific rearrangement.

It has been suggested in another context that slow ligand-induced conformational changes in enzyme structure at the catalytic site could, raise a low activity ground state, E to a higher activity primed, or activated state, E′. This type of mechanism has been invoked to account for sigmoidal relations between enzyme activity and substrate concentration in monomeric proteins [29].

A similar mechanism could lead to activation of the Glut 1 transporter by D-glucose. The model outlined in Scheme 2 shows the unliganded transporter sites as low-, E, or high-energy forms, E′, with the a slow rate of isomerisation between the two forms e.g. $t_{1/2} \approx 5$ ms; at steady state $E'/E = 0.2$. D-Glucose binds rapidly to the transporter with a dissociation constant for ligand A, $K_d = 1$ mM; the isomerisation rate between the low-energy liganded transporter forms, EA and high-energy form, E′A is fast, e.g. $t_{1/2} \approx 0.05$ ms.

The $K_d$ of ligand A for the high-energy form of the transporter is higher ($= 10$ mM) than for the low-energy form; hence as D-glucose also rapidly dissociates from E′A, the proportion of unliganded transporter in the activated state, E′ is raised by low concentrations of D-glucose (Figs. 9 and 10).

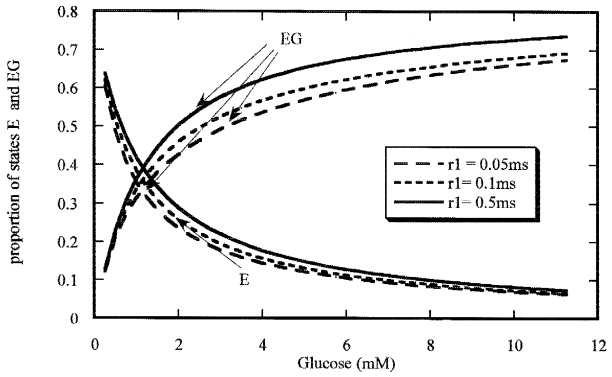


Fig. 9. Simulation of the proportion of states of the transporter with varying external [glucose]. The model parameters are those shown in Scheme 2; where E, EG (Fig. 9) are the unliganded and liganded states of inactive transporter, $K_d = 1$ mM and E′, E′G (Fig. 10) are the unliganded and liganded stated of the activated transporter, $K_d = 10$ mM. The dissociation constants are maintained during the simulation of temperature reduction. The rates of isomerisation between E and E′ are varied; 0.05, 0.1 and 0.5 ms. The rates of association and dissociation of the ligand with all states and the rate of isomerisation of EG and E′G are all $> 10\times$ faster than the fastest rate of isomerisation between E and E′. When the isomerisation rate between E and E′G is slow, i.e. 0.05 ms, low concentrations of D-glucose increase the proportion of the state E′; however, when the isomerisation rate is faster no increase in E′ is obtained.

Another ligand, S, interacting with the transporter immediately after dissociation of $E'A \Rightarrow E' + A$ and prior to decay from E′ to the ground state, E will have a higher probability of reacting with this more mobile form than is the case without priming by a ‘good’ substrate. If the new ligand is a ‘poor’ substrate, e.g. L-sorbose, which by itself does not pro-

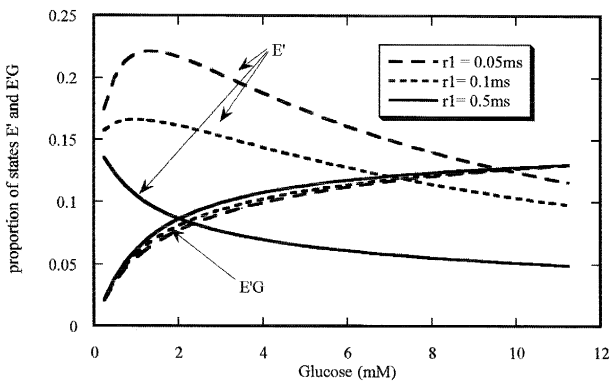


Fig. 10. See legend to Fig. 9.

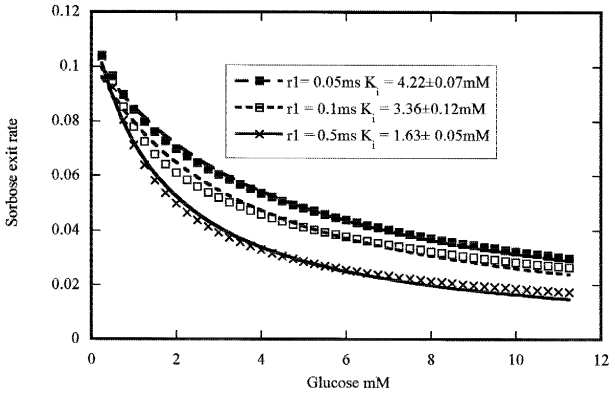


Fig. 11. Simulation of the effects of temperature on the glucose dependent inhibition of sorbose flux. As shown in Scheme 2, the activated form of transporter bound to sorbose, E′S is assumed to have twice the mobility of the inactive form, ES; hence, with low [glucose] present the mobility of sorbose is proportional to (ES + 2 E′S) or (E + 2 E′) tends to be enhanced; however, as [glucose] is raised, the proportion of EG and E′G increases; thereby reducing the overall proportion of free carrier forms, E′ and E, so sorbose transport is inhibited overall. The data points are the simulated rates of net sorbose flux at varying [glucose]; the lines through the points are the non-linear fits to the simulation using the competitive inhibition formulation. $K_i \cdot V_o / (K_i + [G])$. The $K_i$ values ± S.E.M. obtained are presented in the inset in the diagram. Slow isomerisation rates between E and E′ give higher observed $K_i$ values than the faster rates.

mote activation, then co-existence of low concentrations of D-glucose in the bathing solution will raise the probability of L-sorbose binding to the activated state, S + E′ ⇒ E′S; hence L-sorbose flux will not be reduced as much as expected on the basis of simple competitive inhibition between D-glucose and L-sorbose for a single site, E.

The solutions to the model shown in Scheme 2 (Figs. 9–11) were obtained using STELLA II, a simulation program for Macintosh (High Performance Systems Inc., Hanover, NH). The equations for the relative probabilities of the states of the transporter were obtained by numerical solution, either with Runge Kutta or Euler methods (step length 25 ns). Since the turnover number of the glucose transporter is about 1000 $s^{-1}$ at 40°C the assumption is made that the liganded states have a transient lifetime of ≈ 1 ms — so ligand association/dissociation is simulated with a sinwave of frequency 1000 Hz. This was adjusted to give a maximum positive amplitude in proportion to [glucose] and a minimum = zero. Sorbose binding was simulated with an similar periodic signal but a coswave in antiphase to the glucose signal the amplitude was kept very small so that it would not materially interfere with glucose binding in accord with the high $K_m$ of L-sorbose transport [1]. In practice neither the phase nor frequency of the [glucose] or [sorbose] signals made much difference; steady-state solutions of the proportion of transporter states gave qualitatively similar results to those with produced with periodic functions.

The model provides a simple explanation for the rise in $K_i$ of D-glucose- and D-mannose-dependent inhibition of L-sorbose exit as the temperature is reduced (Fig. 11). The rate of decay of the activated state E′ to E is retarded on cooling; hence, higher

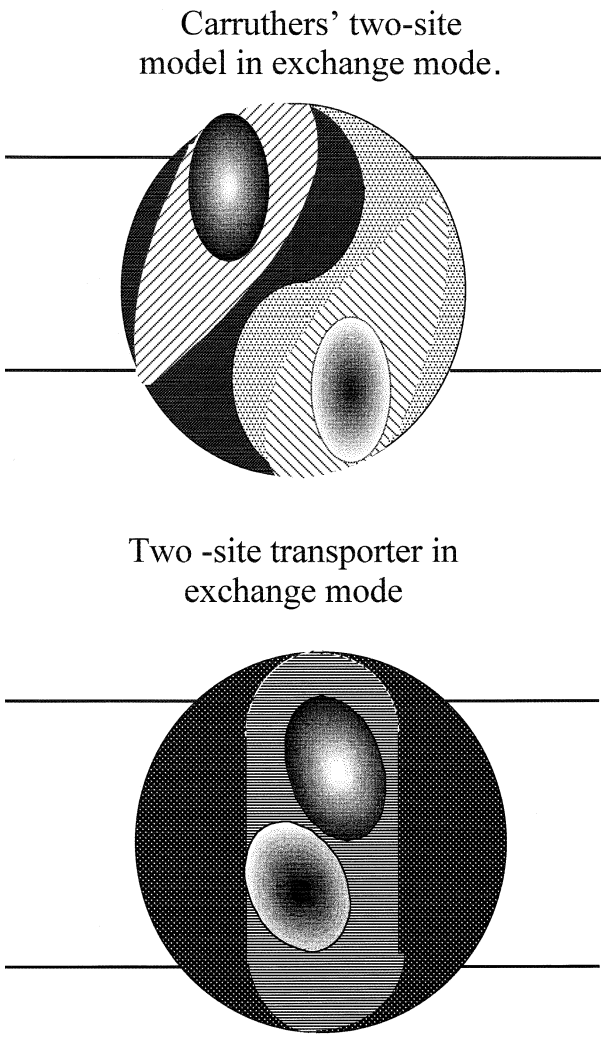


Scheme 3. The two-site variants for exchange transport.

proportions of the transporter remain in states E′ so a larger proportion of the activated state E′S is formed at lower temperatures. This accounts both for the rise in $K_{i(sorbose)}$ of D-glucose and D-mannose on cooling and also accounts for the D-glucose-dependent decrease in the activation energy $E_a$ of L-sorbose exit.

The view that substrate-induced conformation changes may persist as a transient metastable state has been recently invoked to explain how enzyme specificity is linked to conformational differences between the reactive complex for a good substrate and the related complex for a poor one [30].

### *4.5. Accelerated exchange transport*

The model described above also provides a basis for explaining *accelerated exchange* between two 'good' substrates; e.g. D-Glucose and D-glucose, or D-glucose and D-mannose.

The temperature dependencies of human erythrocyte *net* and *exchange* D-glucose transport have been investigated several times. It is commonly found that the $E_a$ for *net entry* is 90–110 kJ/mol [20,21]; whereas for *net exit*, the $E_a$ is between 40 and 60 kJ/mol [3,13,31]. Where comparisons of $E_a$ of *net* D-glucose entry and *exchange* have been made, the $E_a$ of *exchange* is lower by about 60% than $E_a$ for net uptake [13,21,28]. Additionally, van't Hoff plots show that the temperature coefficient of exchange flux in human and rat erythrocytes is much less than for net flux of D-glucose [13,21], i.e. the $\Delta H$ and $\Delta S$ of D-glucose exchange interactions are much less than for D-glucose net flux interactions.

Thus, the main characteristics of exchange transport *viz*: a higher $V_m$ (2–3-fold) and $K_m$ (10–15 mM) than net flux for both influx and efflux at temperatures below 35°C are already incorporated in the model above; namely the higher mobility and $K_d$ of the activated state, E′A than the basal state EA. If, instead of a poor substrate like L-sorbose, the alternate ligand is a 'good' substrate, like D-glucose or D-mannose, then the exchange transport event can viewed either as a simultaneous process, in which the sugars at the inner and outer sites exchange their relative positions [15]; or, as Carruthers and colleagues [32,33] have suggested, the two exchanging ligands bind to linked a pair of alternating transporters whose anti-parallel movements are coupled (Scheme 3). Although, neither mechanism is kinetically distinguishable at present, both two-site variants have the advantage over the one-site model that they account for net transport kinetics and thermodynamics without requiring an energy source for return of the empty transporter.

The lower activation energy of exchange and the also the lower enthalpy and entropy indicate that exchange transport closely resembles L-sorbose with D-glucose present; i.e. the transport is mainly determined via the activated mode and this depends on prior interaction with a good substrate.

## Acknowledgements

The author is grateful to Mr. Mustafa A. Arain for assistance during a summer studentship and to Mr. Robert Roberts for technical help.

## References

[1] P.G. LeFevre, G.F. McGinniss, J. Gen. Physiol. 44 (1960) 87–103.
[2] W.F. Widdas, J. Physiol. 125 (1954) 163–180.
[3] D.M. Miller, Biophys. J. 8 (1968) 1329–1338.
[4] A.K. Sen, W.F. Widdas, J. Physiol. 160 (1962) 404–416.
[5] M. Levine, S. Levine, N.M. Jones, Biochim. Biophys. Acta 255 (1971) 191–300.
[6] J.E.G. Barnett, G.D. Holman, K.A. Munday, Biochem. J. 131 (1973) 211–221.
[7] W.F. Widdas, G.F. Baker, Cytobios 66 (1990) 179–204.
[8] P. LaCelle, H. Passow, J. Membr. Biol. 4 (1971) 270–283.
[9] R.J. Naftalin, G.D. Holman, in: J.C. Ellory, V.L. Lew (Eds.), Membrane Transport in Red Cells, Academic Press, New York, 1977, pp. 257–300.
[10] A. Carruthers, D.L. Melchior, Biochim. Biophys. Acta 728 (1983) 254–266.
[11] A.K. Sen, W.F. Widdas, J. Physiol. 160 (1962) 393–403.
[12] P.G. LeFevre, J.K. Marshall, Am. J. Physiol. 194 (1958) 333–337.
[13] R.R. Whitesell, D.M. Regen, A.H. Beth, D.K. Pelletier, N.A. Abumrad, Biochemistry 28 (1989) 5618–5625.
[14] C.Y. Jung, L.M. Carlson, D.A. Whaley, Biochim. Biophys. Acta 241 (1971) 613–627.
[15] R.J. Naftalin, R.J. Rist, Biochim. Biophys. Acta 1191 (1994) 65–78.
[16] E.M. Wright, N. Bindslev, J. Membr. Biol. 29 (1976) 289–312.
[17] W.R. Galey, J.D. Owen, A.K. Solomon, J. Gen. Physiol. 61 (1973) 727.

[18] R. Krupka, Biochemistry 10 (1971) 1143–1147.
[19] A.C. Dawson, W.F. Widdas, J. Physiol. 168 (1963) 644–659.
[20] F. Bowyer, W.F. Widdas, J. Physiol. 141 (1958) 219–232.
[21] J. Brahm, J. Physiol. 339 (1983) 339–354.
[22] A.G. Lowe, A.R. Walmsley, Biochim. Biophys. Acta 857 (1986) 146–154.
[23] C.Y. Jung, A.L. Rampal, J. Biol. Chem. 252 (1977) 5456–5463.
[24] D.C. Sogin, P.C. Hinkle, Biochemistry 19 (1980) 5417–5420.
[25] J.R. Appleman, G.E. Leinhard, Biochemistry 28 (1989) 8221–8227.
[26] J.M. May, J.M. Beechem, Biochemistry 32 (1993) 2907–2915.
[27] A.R. Walmsley, A.G. Lowe, P.J.F. Henderson, Eur. J. Biochem. 221 (1994) 513–522.
[28] A. Janoshazi, A.K. Solomon, J. Membr. Biol. 132 (1993) 167–178.
[29] A. Cornish-Bowden, M.L. Cardenas, J. Theor. Biol 124 (1987) 1–23.
[30] C.B. Post, W.J. Ray, Biochemistry 34 (1995) 15881–15885.
[31] B.L. Hankin, W.D. Stein, Biochim. Biophys. Acta 288 (1972) 127–136.
[32] P.E. Coderre, E.K. Cloherty, R.J. Zottola, A. Carruthers, Biochemistry 34 (1995) 9762–9773.
[33] R.J. Zottola, E. Cloherty, P.E. Coderre, A. Hansen, D.N. Hebert, A. Carruthers, Biochemistry 34 (1995) 9734–9747.